Nanoscale Res Lett (2009) 4:779–788
DOI 10.1007/s11671-009-9338-2

NANO REVIEW

One-Dimensional Nanostructures and Devices of II–V Group Semiconductors

Guozhen Shen · Di Chen

Received: 12 April 2009 / Accepted: 24 April 2009 / Published online: 15 May 2009

Abstract The II–V group semiconductors, with narrow band gaps, are important materials with many applications in infrared detectors, lasers, solar cells, ultrasonic multipliers, and Hall generators. Since the first report on trumpet-like Zn_3P_2 nanowires, one-dimensional (1-D) nanostructures of II–V group semiconductors have attracted great research attention recently because these special 1-D nanostructures may find applications in fabricating new electronic and optoelectronic nanoscale devices. This article covers the 1-D II–V semiconducting nanostructures that have been synthesized till now, focusing on nanotubes, nanowires, nanobelts, and special nanostructures like heterostructured nanowires. Novel electronic and optoelectronic devices built on 1-D II–V semiconducting nanostructures will also be discussed, which include metal–insulator-semiconductor field-effect transistors, metal-semiconductor field-effect transistors, and *p*–*n* heterojunction photodiode. We intent to provide the readers a brief account of these exciting research activities.

Keywords Nanowires · Nanotubes · Nanobelts · Semiconductors · Nanoelectronics

Introduction

Because of the ability to synthesize them in numerous configurations and their unique physical, chemical, optical, electrical, and magnetic properties, one-dimensional (1-D) nanostructures have attracted great interest in recent years [1–5]. 1-D nanostructures play important roles both as interconnect and functional units in fabricating nanoscale electronic, optoelectronic, electrochemical, and electromechanical devices. 1-D nanostructures have been synthesized for a lot of materials, including metals, II–VI and III–V semiconductors, sulfides, nitrides, etc., using a variety of synthetic techniques, such as solution process, vapor–solid process, vapor–liquid–solid process, template-directed process and so on [6–40].

Semiconducting II–V compounds are important narrow band gap semiconductors with great scientific and technological importance [41]. They are suggested to exhibit pronounced size quantization effects due to the large excitonic radii. Bulk II–V semiconductors have been used as infrared detectors, lasers, solar cells, ultrasonic multipliers, and Hall generators [42–50]. However, research on nanoscale II–V semiconductors, especially 1-D nanostructures, has been lingering far behind compared with the significant progress in the studies of 1-D II–VI and III–V semiconductors, mainly due to the significant synthetic experimental difficulties, such as lack of generalized synthetic methodologies, instability in air, etc. Since the first successfully synthesized trumpet-like Zn_3P_2 nanowires in 2006, many kinds of interesting 1-D II–V semiconductors nanostructures have been reported using different techniques, which greatly promote their further application in nanoscale electronic and optoelectronic devices.

This article will provide a comprehensive review of the state-of-the-art research activities focused on synthesis and devices of 1-D II–V semiconducting nanostructures. The first section introduces typical 1-D nanostructures obtained on II–V semiconductors, including nanotubes,

G. Shen (✉) · D. Chen
Wuhan National Laboratory for Optoelectronics and College of Optoelectronic Science and Technology, Huazhong University of Science and Technology, Wuhan 430074, People's Republic of China
e-mail: gzshen@mail.hust.edu.cn; guozhens@gmail.com

nanowires, nanobelts, and some special nanostructures. Next, some important electronic and optoelectronic devices built on 1-D II–V semiconducting nanostructures are presented, which include metal–insulator-semiconductor field-effect transistors (MIS-FET), metal-semiconductor field-effect transistors (MS-FET), and *p–n* heterojunction photodiode. This review will then conclude with some personal perspectives and outlook on the future developments in the 1-D II–V semiconducting nanostructures research area.

Typical 1-D Nanostructures of II–V Group Semiconductors

Since the first successfully synthesized trumpet-like Zn_3P_2 nanowires in 2006, many kinds of interesting 1-D II–V semiconducting nanostructures, such as nanotubes, nanowires, and nanobelts, special nanostructures have been reported using different techniques. In this section, we will discuss several typical 1-D nanostructures obtained on II–V semiconductors.

Nanotubes

Considerable attention has been paid on semiconducting nanotubes since the first report of carbon nanotubes by Iijima in 1991 [11]. Nanotubes are often obtained for materials with layered or pseudolayered structures [13]. Without these kinds of structures, templates (hard templates or soft templates) are usually used to promote the formation of tubular structures [21, 51]. Recently, we developed an in situ nanorod template method to synthesize high-quality single crystalline II–V nanotubes, including Zn_3P_2 nanotubes and Cd_3P_2 nanotubes [52]. The whole process can be expressed as shown in Fig. 1. This process was performed in a vertical induction furnace at high temperature and the mixture of ZnS (or CdS), Mn_3P_2 and P powders were used as the evaporation sources. At high reaction temperature, ZnS or CdS was evaporated and reacted with graphite to generate Zn or Cd vapors, which were transferred to low temperature region and deposited on the surface of graphite crucible, resulted in the formation of Zn or Cd nanorods due to the anisotropic nature of wurtzite Zn or Cd phases. At the same time, Mn_3P_2 was thermally decomposed to generate P gases. These newly generated P gases deposited on the surface of Zn or Cd nanorods and reacted with them to generate the Zn_3P_2 or Cd_3P_2 shells. After a reaction time, the inner Zn or Cd nanorods were consumed and finally only Zn_3P_2 or Cd_3P_2 nanotubes were formed.

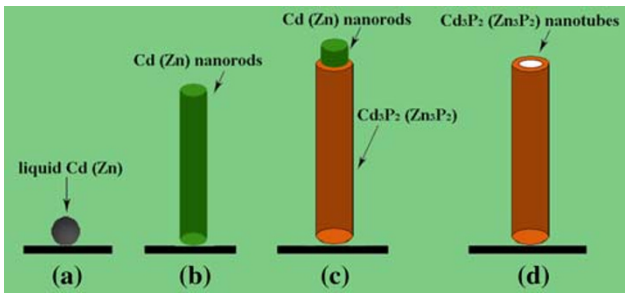

Fig. 1 Schematic illustration showing the formation of II–V nanotubes via the in situ nanorod template method

Figure 2a is a SEM image of the Cd_3P_2 product obtained in the in situ nanorod template process. 1-D nanostructures can be found deposited on the graphite crucible on a large scale. A magnified SEM image shown inset clearly reveals that they are hollow nanotubes. Figure 2b and c show typical TEM images of the obtained Cd_3P_2 nanotubes. The clear brightness contrast confirms that they are hollow nanotubes. Typical nanotubes have diameters of about 100 nm and the wall thickness of several nanometers. As-synthesized Cd_3P_2 nanotubes are of single crystalline nature with the preferred growth direction perpendicular to the (101) planes as revealed in Fig. 2d. Similarly, the Zn_3P_2 products obtained in the in situ template process are also single crystalline nanotubes as shown in Fig. 2e. We should mention that defects existed in the as-synthesized Cd_3P_2 and Zn_3P_2 nanotubes because of the release of built-in strain.

Nanowires

Nanowire is one of the most common 1-D structure and many kinds of materials can form into the nanowire structures. Till now, Cd_3P_2, Zn_3P_2, and Cd_3As_2 among the II–V group semiconductors were found to be able to form into the nanowire structures. Omari et al. [53] reported the synthesis of single-crystalline Cd_3As_2 nanowires by thermal evaporation of Cd_3As_2 powders at 750 °C. Figure 3a is a SEM image of the Cd_3As_2 nanowires. Studies found that these Cd_3As_2 nanowires are single crystals with the growth directions along the (112) crystal planes. Omari et al. also investigated the optical properties of these nanowires and found that they have IR active direct type absorption transitions at 0.11, 0.28, and 0.54 eV, which make it possible to use these nanowires as low cost optoelectronic devices and photodetectors operating in the long wavelength range.

Liu et al. [54] reported the synthesis of Zn_3P_2 nanowires by the reaction between Zn and InP powders at 850 °C. These Zn_3P_2 nanowires are also single crystals and have typical diameters of about 100 nm and lengths of tens of microns, as revealed in Fig. 3b. During this process, Au

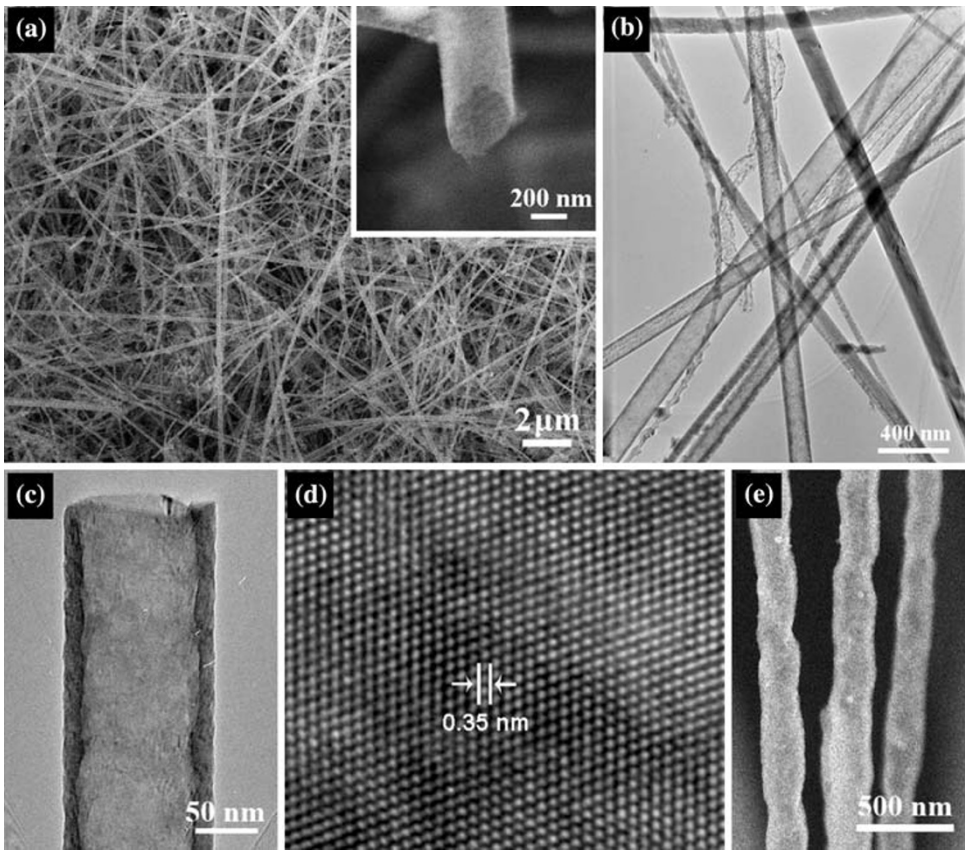

Fig. 2 **a** SEM image; **b**, **c** TEM image; and **d** HRTEM image of Cd_3P_2 nanotubes. **e** SEM image of Zn_3P_2 nanotubes

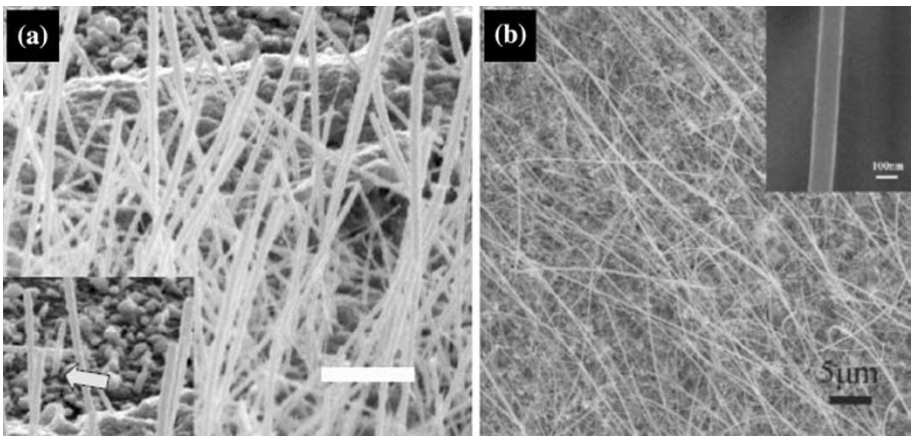

Fig. 3 SEM images of: **a** Cd_3As_2 nanowires and **b** Zn_3P_2 nanowires

was used as catalysts to direct the nanowire growth and it is obviously a vapor–liquid–solid (VLS) process.

Nanobelts

We were able to synthesize high quality Zn_3P_2 and Cd_3P_2 nanobelts on a large scale using a method similar to the synthesis of Zn_3P_2 and Cd_3P_2 nanotubes [55]. Zn_3P_2 and Cd_3P_2 nanobelts were synthesized by using a mixture of ZnS (or CdS) and Mn_3P_2 powders as the evaporation source. The reaction was performed at 1350 °C for about 1 h. Figure 4a is a SEM image of the synthesized Zn_3P_2 nanobelts with rectangular cross-sections, which have diameters of about 100–200 nm and thickness of 40 nm. A TEM image of a single Cd_3P_2 nanobelt is depicted in Fig. 4b. The twisted structure confirms it is a nanobelt and the thickness is about 70 nm. The microstructures of the Cd_3P_2 nanobelts were studied by HRTEM and SAED. Figure 4c and d are the HRTEM images taken from the surface and body of a Cd_3P_2 nanobelt, respectively.

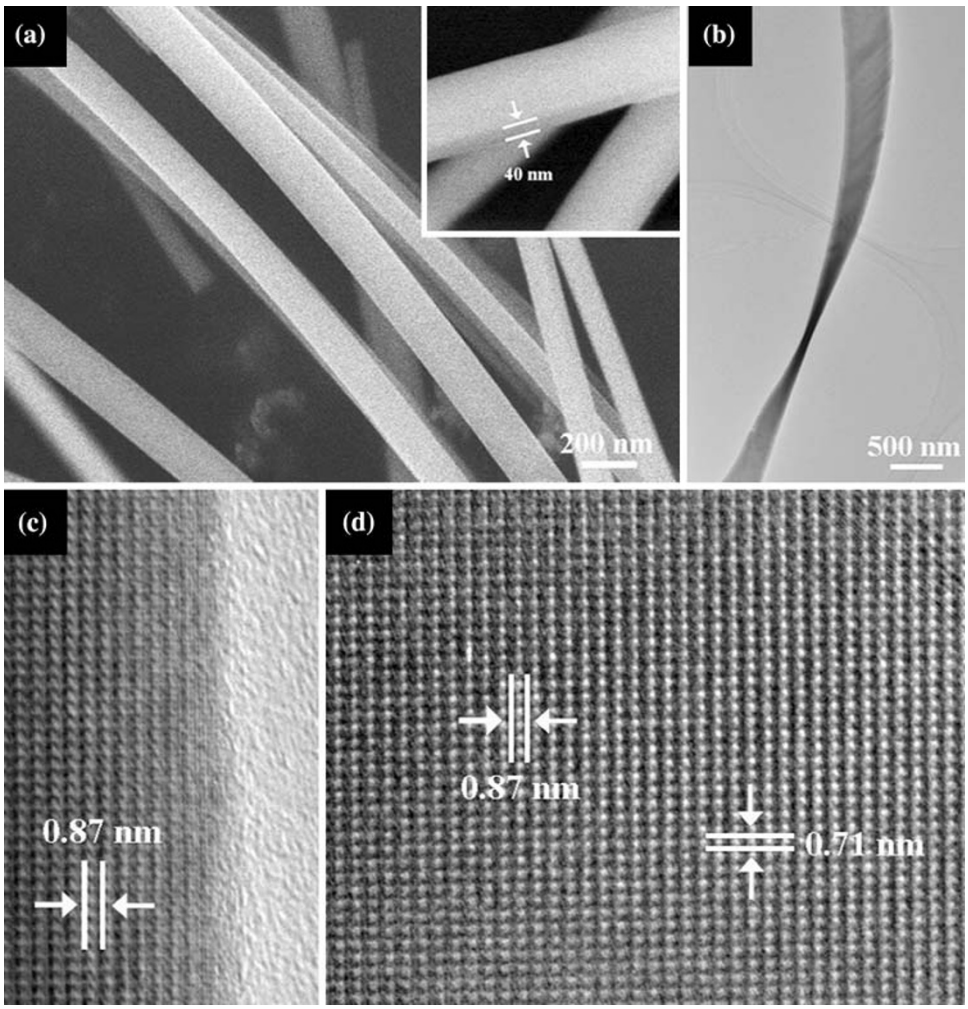

Fig. 4 **a** SEM image of Zn_3P_2 nanobelts. **b** TEM image and **c**, **d** HRTEM images of Cd_3P_2 nanobelts

The clearly resolved lattice fringes perpendicular to and along the longitudinal axis of the nanobelt are 0.71 and 0.87 nm, respectively, corresponding to the (101) and (010) lattice planes of tetragonal Cd_3P_2 phase. Studies revealed that these Cd_3P_2 nanobelts have the preferred growth directions along the [010] crystallographic orientations. For the synthesis of Zn_3P_2 and Cd_3P_2 nanobelts, no catalyst was used, indicating that it was governed by the vapor–solid (VS) mechanism. In fact, we found that Zn_3P_2 and Cd_3P_2 nanobelts can also be synthesized via the VLS mechanism if suitable catalysts, such as indium, were selected.

Special 1-D Nanostructures

Synthesis and assembly of 1-D nanostructures with special morphologies, shapes, and compositions have attracted great interests very recently because they may process interesting physical and chemical properties associated with their specific characteristics. They may also be used to fabricate special electronic and optoelectronic devices which cannot be fulfilled using simple 1-D nanostructures.

Wang et al. [56] recently succeeded in synthesizing three-dimensional (3-D) branched tree-like Zn_3P_2 nanostructures as shown in Fig. 5. These 3-D Zn_3P_2 nanostructures were synthesized in a thermal-assisted pulse-laser-deposition (PLD) system using Zn_3P_2/ZnO/Zn as the target. A top view image shown in Fig. 5a demonstrated that these 3-D nanostructures have a sixfold symmetry. The tree-like branched shapes were confirmed by the side view SEM image depicted in Fig. 5b. The constituent branches of the tree-like structures were found to be as long as several tens of micrometers, with the diameters lying in the range of ten to several hundred nanometers. During this process, it was found that nanobelts were formed once the branches grew much longer as indicated in Fig. 5c. The composition of the tree-like Zn_3P_2 structures was checked using energy-dispersive spectrometry (EDS) and the results confirm they are pure Zn_3P_2 (Fig. 5d).

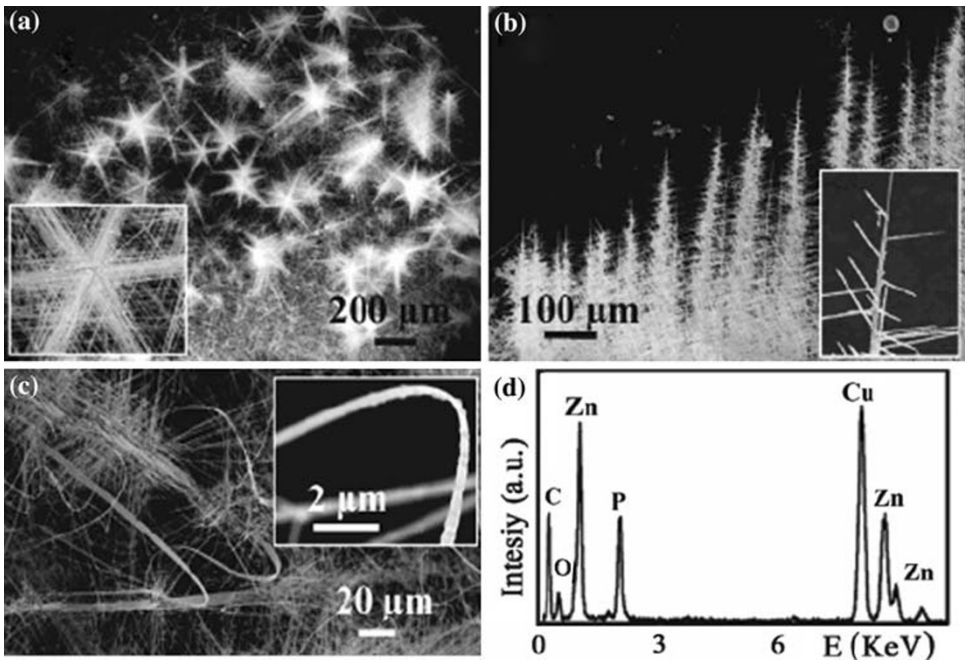

Fig. 5 **a**–**c** SEM images and **d** EDS spectrum of tree-like branched Zn_3P_2 nanostructures

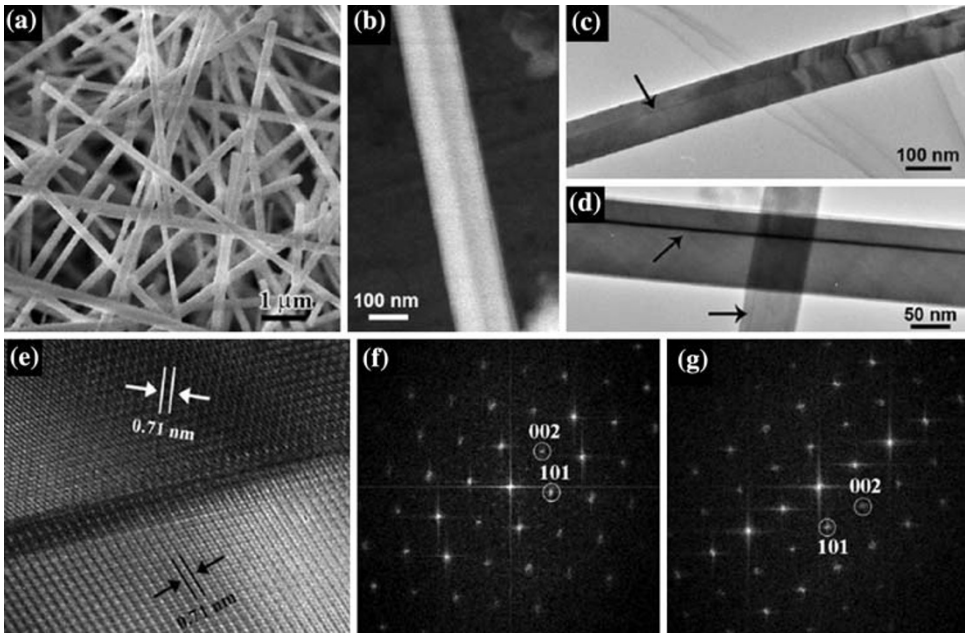

Fig. 6 **a**, **b** SEM images; **c**, **d** TEM images of bicrystal Zn_3P_2 nanobelts. **e** HRTEM image and **f**, **g** FFT patterns of bicrystal Cd_3P_2 nanobelts

1-D bicrystalline nanostructures have received great attention because of their peculiar structures and structure-related properties. Several kinds of 1-D bicrystalline nanostructures have been obtained for ZnS, InP, etc. [57–62]. We synthesized bicrystalline Zn_3P_2 and Cd_3P_2 nanobelts via a VS process in the vertical induction furnace system [63]. The source materials used are a mixture of Zn (or Cd), ZnS (or CdS), GaP, and Mn_3P_2 powders. Figure 6a is a SEM image of the Zn_3P_2 product, which clearly shows that long and straight nanobelts are obtained on a large scale. Each nanobelt has a uniform width of 100–200 nm and length in the range of tens of micrometers. A high-magnification SEM image shown in Fig. 6b clearly reveals that these nanobelts are bicrystals with distinct grain boundary along the direction parallel to the growth direction. TEM images of several typical Zn_3P_2 bicrystal nanobelts were depicted in Fig. 6c and d. Grain boundaries were clearly observed in the middle of the nanobelts, indicating the bicrystal nature. These Zn_3P_2 bicrystal nanobelts are composed of two single-crystal with the

preferred growth axis along the [101] directions. HRTEM image taken from a single Cd_3P_2 bicrystal nanobelt was shown in Fig. 6e. The marked lattice fringes in each part of the Cd_3P_2 nanobelt are 0.71 nm, in accordance with the (101) plane of tetragonal Cd_3P_2. The correspondence Fast Fourier Transform (FFT) patterns taken from the two parts within a single bicrystal nanobelt were demonstrated in Fig. 6f and g, which verified the formation of bicrystalline Cd_3P_2 nanobelts with the preferred growth along the [101] directions.

Besides the above discussed special 1-D II–V semiconducting nanostructures, we were also able to get other kinds of interesting 1-D II–V semiconducting nanostructures. For instance, Fig. 7a and b show the SEM and TEM image of zigzag twinned Zn_3P_2 nanowires, which were also obtained in the vapor phase process [64]. Spherical indium

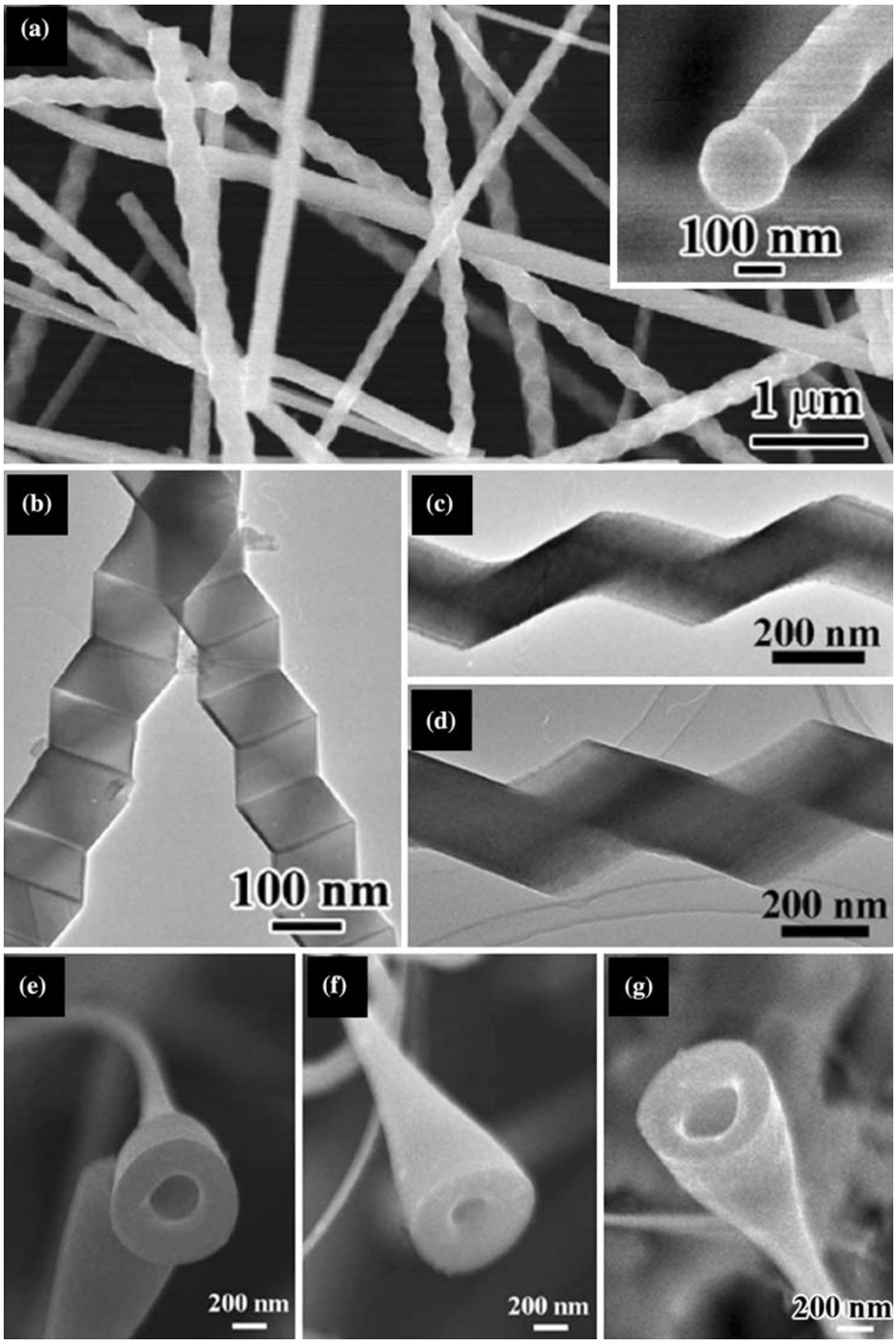

Fig. 7 **a** SEM image and **b** TEM image of zigzag twinned Zn_3P_2 nanowires. **c**, **d** TEM image of zigzag single-crystal Zn_3P_2 nanowires. **e**–**g** Typical SEM image of trumpet-like Zn_3P_2 nanowires

nanoparticles were found attached to the zigzag nanowires, indicating that the process was governed by the VLS mechanism. These zigzag Zn_3P_2 nanowires typically have periodic twins with a period of 50–120 nm along the whole nanowires. Lots of defects were found in the twin boundaries area, similar to previous reports on twinned nanowires [57–62]. If we did not use indium catalysts and kept other conditions constant, we synthesized zigzag single crystal Zn_3P_2 nanowires as shown in Fig. 7c and d. The angle between two neighboring kinks is about 120°, consistent with that between the (001) and (101) planes of tetragonal Zn_3P_2 phase. Figure 7e–g are SEM images of trumpet-like Zn_3P_2 nanowires, which are composed of a hollow cone supported by a nanowire [65]. The trumpet-like Zn_3P_2 nanowires are single crystals with preferred growth directions along the [010] orientations. Other special II–V semiconducting 1-D nanostructures include 1-D hierarchical Zn_3P_2/ZnS nanotube/nanowires heterostructures, which consist of main Zn_3P_2 nanotube wrapped with high density ZnS nanowires [66].

We have discussed above several kinds of 1-D II–V semiconducting nanostructures obtained till now. By carefully controlling the experimental parameters, such as evaporation sources, temperature, carrier gases, etc., more 1-D nanostructures are expected to be obtained for II–V group semiconductors.

Device Applications of 1-D II–V Semiconducting Nanostructures

As an important group of narrow band gap semiconductors, 1-D II–V semiconducting nanostructures can be used to fabricate nanoscale electronic and optoelectronic devices. Several kinds of nanodevices had been fabricated built on single 1-D II–V semiconducting nanostructure, such as MIS-FET, MS-FET, and *p–n* heterojunction photodiode.

MIS-FET Built on Single 1-D II–V Semiconducting Nanostructures

Figure 8a inset is a schematic illustration of a MIS-FET built on a single Zn_3P_2 nanowire. Basically, the MIS-FET is supported on an oxidized *p*-type silicon substrate with the underlying conducting silicon as the back gate electrode to vary the electrostatic potential of the nanostructure. Two metal contacts, such as Au and Ti/Au, corresponding to the source and drain electrodes, are defined by either photolithography or electron beam lithography, followed by evaporation of suitable metal contacts. The I_{ds}–V_{ds} curves of the MIS-FET are illustrated in Fig. 8a, showing typical *p*-type behavior of the Zn_3P_2 nanowire. From the I_{ds}–V_{ds} measurement, the resistivity of the nanowire is calculated to be about 1.96 Ωcm. We also built MIS-FET using zigzag

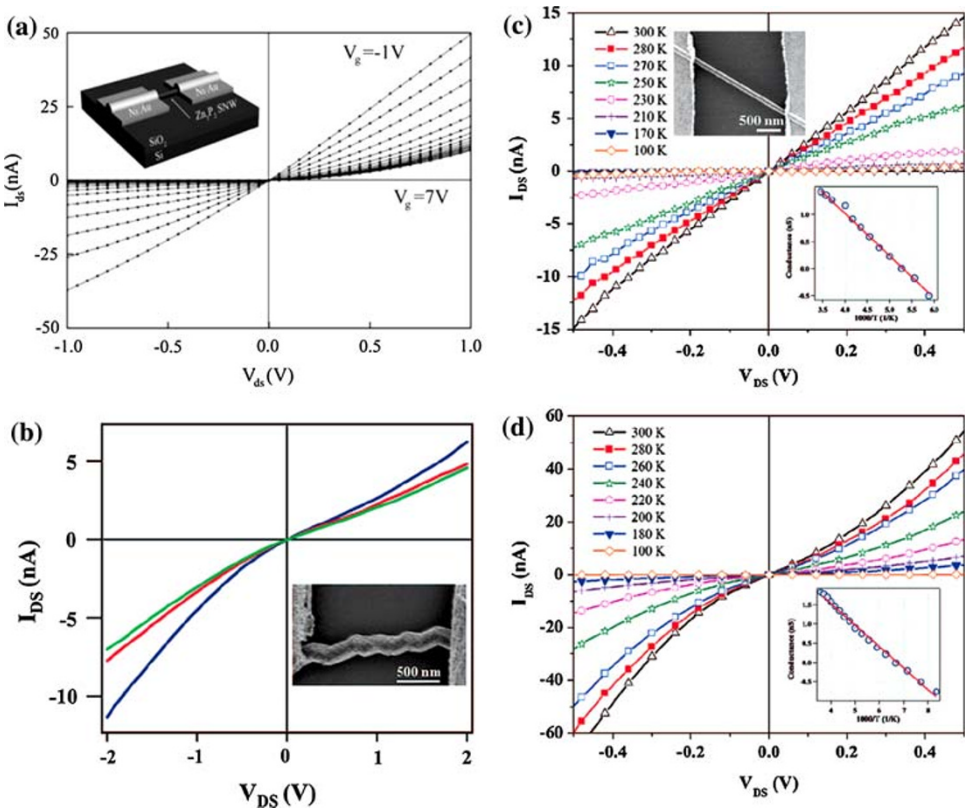

Fig. 8 **a** I_{ds}–V_{ds} characteristics of Zn_3P_2 nanowire MIS-FET under gate bias ranging from −1 V to 7 V with a step of 0.5 V. The inset is a schematic illustration of the device. **b** I_{ds}–V_{ds} characteristics of single zigzag Zn_3P_2 nanowire-based MIS-FET, showing *p*-type behavior. *I–V* curves of **c** Zn_3P_2 and **d** Cd_3P_2 nanobelts measured at 300–100 K. The insets show the conductance in a logarithmic scale at zero bias voltage plotted as a function of 1000/T

Zn_3P_2 nanowire as shown in Fig. 8b inset. As-fabricated MIS-FET also confirms the *p*-type behavior of the zigzag nanowire.

To investigate the electronic transport behaviors of 1-D II–V semiconducting nanostructures, we fabricated MIS-FET built on single Zn_3P_2 and Cd_3P_2 bicrystal nanobelts and explored the electronic transport behaviors as a function of temperature in vacuum [63]. A SEM image of the Zn_3P_2 MIS-FET is depicted in Fig. 8c inset. Figure 8c displays the I–V curves of a Zn_3P_2 bicrystal nanobelt MIS-FET device measured in the temperature region of 100–300 K without applying gate voltage. The conductance of the device continuously decreased as the temperature decreased. The zero-bias conductance at 300 K is calculated to be 27.75 nano-Siemens (nS) and it decreases to 0.01 nS at 100 K. Plotted the zero-bias conductance in a logarithmic scale as a function of 1000/T gives a linear behavior within the temperature region investigated. All these results suggested that the thermal activation of carriers is the dominant transport mechanism for the Zn_3P_2 bicrystal nanobelt MIS-FET. The electronic transport behavior of Cd_3P_2 bicrystal nanobelts was also investigated at different temperatures and the results (Fig. 8d) also suggested a dominant thermal activation of carriers transport mechanism.

MS-FET Built on Single 1-D II–V Semiconducting Nanostructures

Liu et al. [67] fabricated MS-FET using single Zn_3P_2 nanowire as the active material. Basic structure of the MS-FET is demonstrated in Fig. 9a, in which Ni/Au was used as electrodes and Al as the top gate electrode across the nanowire. The typical I_{SD}–V_{SD} characteristics of a *p*-type Zn_3P_2 nanowire based MS-FET measured at room temperature under gate biases ranging from −0.5 to 0 V with a step of 0.1 V is depicted in Fig. 9b. As-fabricated MS-FET shows *p*-type conductance behavior and it is turned off at zero gate bias, indicating that the MS-FET was in the E-mode.

p–*n* Heterojunction Photodiode Built with Zn_3P_2 Nanowires and ZnO Nanowires

Very recently, Wang et al. fabricated *p*–*n* heterojunction photodiode using a crossed heterojunction made of *p*-type Zn_3P_2 nanowire and *n*-type ZnO nanowire [56]. The device structure is displayed in Fig. 10a inset and the I–V curve at reverse and forward bias is illustrated in Fig. 10. Wang et al. studied the device behaviors by checking the photodiode under reverse bias and in the dark and under the illumination of light with wavelength of 532 or 680 nm. The results are presented in Fig. 10b, which show apparent

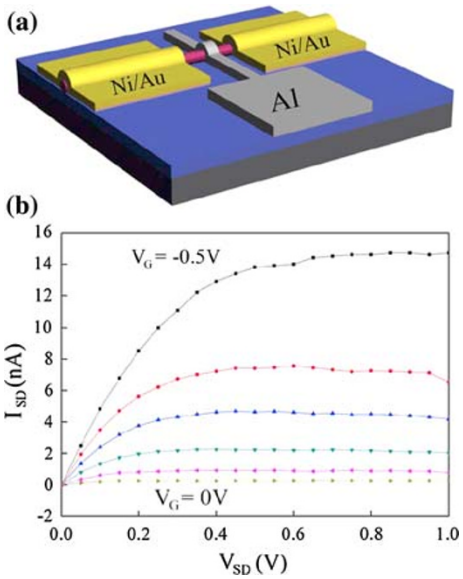

Fig. 9 **a** Schematic illustration of a Zn_3P_2 nanowire based MS-FET. **b** I_{SD}–V_{SD} characteristics of a *p*-type Zn_3P_2 nanowire based MS-FET measured at room temperature under gate biases ranging from −0.5 to 0 V with a step of 0.1 V

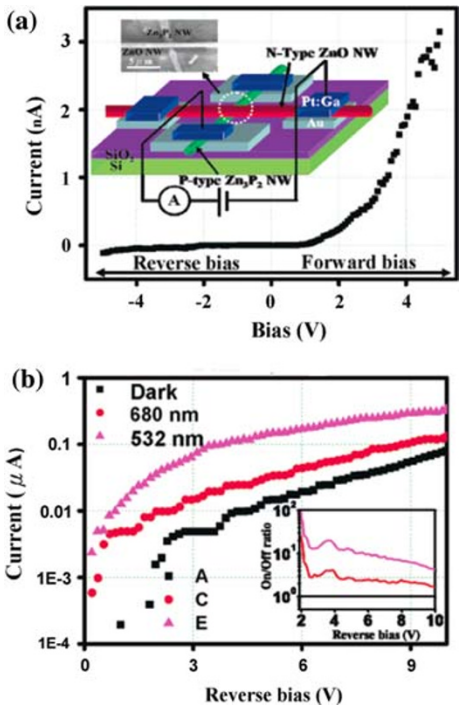

Fig. 10 **a** *I*–*V* curve for ZnO/Zn_3P_2 nanoscale heterojunction at reverse and forward bias. Inset shows the prototype of the nanodevice. **b** *I*–*V* curve of ZnO/Zn_3P_2 heterojunction under illumination of different wavelengths as displayed in logarithmic scale under reverse bias

current enhancement by the light. The increase of the current results from the generation of electron-hole pairs inside the depletion region and nearby under the excitation

of the light. The *p–n* heterojunction photodiode gives rapid response and very high on/off ratio upon light illumination.

Conclusion

In conclusion, we provide a comprehensive review of the state-of-the-art research activities focused on the synthesis and device applications of 1-D II–V semiconducting nanostructures. The rapid expended achievements, till now, toward 1-D II–V semiconducting nanostructures should inspire more and more research efforts to address the remaining challenges in this interesting filed.

Although comprehensive efforts have been made toward the synthesis of high-quality 1-D II–V semiconducting nanostructures, there is still plenty of room left unexploited. We believe that future work should continue to focus on generating them in more controlled, predictable, and simple ways. The II–V semiconductors exhibit pronounced size quantization effects due to the large excitonic radii, thus, it is important to synthesize 1-D II–V semiconducting nanostructures with diameters smaller than the excitonic radii. For example, one needs to find ways to get II–V semiconducting nanotubes with either very small diameter or very thin wall thickness. The physical and chemical properties of II–V semiconducting nanostructures with diameters smaller than the excitonic radii will then need to be investigated and more interesting results are expected to be gotten soon.

Besides, more functional nanoscale electronic and optoelectronic devices are expected to be built on 1-D II–V semiconducting nanostructures and the performance of the devices will be largely improved with the progress of producing high-quality 1-D II–V semiconducting nanostructures.

Acknowledgment The authors acknowledge financial support from the High-level Talent Recruitment Foundation of Huazhong University of Science and Technology. The authors acknowledge the permission from the corresponding publishers/groups to reproduce their materials, especially figures, used in this paper.

References

1. J. Hu, T.W. Odom, C.M. Lieber, Acc. Chem. Res. **32**, 435 (1999). doi:10.1021/ar9700365
2. Y. Cui, C.M. Lieber, Science **291**, 851 (2001). doi:10.1126/science.291.5505.851
3. G.Z. Shen, Y. Bando, D. Golberg, Int. J. Nanotechnol. **4**, 730 (2007)
4. Y. Xia, P. Yang, Y. Sun, Y. Wu, B. Mayer, B. Gates, Y. Yin, F. Kim, H. Yan, Adv. Mater. **15**, 353 (2003). doi:10.1002/adma.200390087
5. Z.W. Pan, Z.R. Dai, Z.L. Wang, Science **291**, 1947 (2001). doi:10.1126/science.1058120
6. Y. Huang, X. Duan, Q. Wei, C.M. Lieber, Nature **291**, 630 (2001)
7. S.Y. Bae, H. Seo, J. Park, H. Yang, J.C. Park, S.Y. Lee, Appl. Phys. Lett. **81**, 126 (2002). doi:10.1063/1.1490395
8. H.T. Ng, J. Li, M.K. Smith, P. Nguyen, A. Cassel, J. Han, M. Meyyappan, Science **300**, 1249 (2003). doi:10.1126/science.1082542
9. W. Lu, Y. Ding, Y. Chen, Z.L. Wang, J. Fang, J. Am. Chem. Soc. **127**, 10112 (2005). doi:10.1021/ja052286j
10. C.B. Murray, D.J. Norris, M.G. Bawendi, J. Am. Chem. Soc. **115**, 8706 (1993). doi:10.1021/ja00072a025
11. S. Iijima, Nature **354**, 56 (1991). doi:10.1038/354056a0
12. C.R. Martin, Science **266**, 1961 (1994). doi:10.1126/science.266.5193.1961
13. Y. Feldman, E. Wasserman, D.J. Srolovitz, R. Tenne, Science **267**, 222 (1995). doi:10.1126/science.267.5195.222
14. D. Wang, H.J. Dai, Angew. Chem. Int. Ed. Engl. **41**, 4783 (2002). doi:10.1002/anie.200290047
15. J. Golberger, R. He, Y. Zhang, S. Lee, H. Yan, H. Choi, P. Yang, Nature **422**, 599 (2003). doi:10.1038/nature01551
16. B. Gates, Y. Yin, Y. Xia, J. Am. Chem. Soc. **122**, 12582 (2000). doi:10.1021/ja002608d
17. X. Wang, Y.D. Li, Angew. Chem. Int. Ed. Engl. **41**, 4790 (2002). doi:10.1002/anie.200290049
18. J.K. Yuan, W. Li, S. Gomez, S.L. Suib, J. Am. Chem. Soc. **127**, 14184 (2005). doi:10.1021/ja053463j
19. B. Liu, H.C. Zeng, J. Am. Chem. Soc. **125**, 4430 (2003). doi:10.1021/ja0299452
20. G.R. Patzke, F. Krumeich, R. Nesper, Angew. Chem. Int. Ed. Engl. **41**, 2446 (2003). doi:10.1002/1521-3773(20020715)41:14<2446::AID-ANIE2446>3.0.CO;2-K
21. H.J. Fan, M. Knez, R. Scholz, K. Nielsch, E. Pippel, D. Hesse, M. Zacharias, U. Gosele, Nat. Mater. **5**, 627 (2006). doi:10.1038/nmat1673
22. S. Han, C. Li, Z. Liu, B. Lei, D. Zhang, W. Jin, X. Liu, T. Tang, C. Zhou, Nano Lett. **4**, 1241 (2004). doi:10.1021/nl049467o
23. M. Nath, C.N.R. Rao, J. Am. Chem. Soc. **123**, 4841 (2001). doi:10.1021/ja010388d
24. G.Z. Shen, J. Cho, J. Yoo, G. Yi, C.J. Lee, J. Phys. Chem. B **109**, 9294 (2005). doi:10.1021/jp044888f
25. G.Z. Shen, Y. Bando, D. Golberg, Appl. Phys. Lett. **88**, 123107 (2006). doi:10.1063/1.2186980
26. G.Z. Shen, Y. Bando, D. Chen, B. Liu, C. Zhi, D. Golberg, J. Phys. Chem. B **110**, 3973 (2006). doi:10.1021/jp056783y
27. G.Z. Shen, Y. Bando, B. Liu, C. Tang, Q. Huang, D. Golberg, Chem. Eur. J. **12**, 2987 (2006). doi:10.1002/chem.200500937
28. G.Z. Shen, Y. Bando, C. Ye, B. Liu, D. Golberg, Nanotechnology **17**, 3468 (2006). doi:10.1088/0957-4484/17/14/019
29. G.Z. Shen, Y. Bando, B. Liu, D. Golberg, C.J. Lee, Adv. Funct. Mater. **16**, 410 (2006). doi:10.1002/adfm.200500571
30. G.Z. Shen, D. Chen, C.J. Lee, J. Phys. Chem. B **110**, 15689 (2006). doi:10.1021/jp0630119
31. G.Z. Shen, D. Chen, J. Am. Chem. Soc. **128**, 11762 (2006)
32. G.Z. Shen, Y. Bando, J. Hu, D. Golberg, Appl. Phys. Lett. **90**, 123101 (2007). doi:10.1063/1.2716242
33. G.Z. Shen, D. Chen, C. Zhou, Chem. Mater. **20**, 3788 (2008). doi:10.1021/cm8008557
34. G.Z. Shen, P.C. Chen, Y. Bando, D. Golberg, C. Zhou, Chem. Mater. **20**, 6779 (2008). doi:10.1021/cm802042k
35. G.Z. Shen, P.C. Chen, C. Zhou, J. Mater. Chem. **19**, 828 (2009). doi:10.1039/b816543b
36. A. Javey, J. Guo, Q. Wang, M. Lundstrom, H. Dai, Nature **424**, 654 (2003). doi:10.1038/nature01797
37. Z.L. Wang, Adv. Mater. **15**, 432 (2003). doi:10.1002/adma.200390100
38. J. Jung, H. Kobayashi, K.J.C. Van Bommel, S. Shinkai, T. Shimizu, Chem. Mater. **14**, 1445 (2002). doi:10.1021/cm011625e

39. F. Dumestre, B. Chaudret, C. Amiens, M. Respaud, P. Fejes, P. Renaud, P. Zurcher, Angew. Chem. Int. Ed. Engl. **42**, 5213 (2003). doi:10.1002/anie.200352090
40. L. Samuelson, Mater. Today **6**, 22 (2003). doi:10.1016/S1369-7021(03)01026-5
41. O. Madelung, *Data in science and technology: semiconductors other than group IV elements and III–V compounds* (Springer, Berlin, Germany, 1991)
42. W. Zdanowicz, L. Zdanowicz, Annu. Rev. Mater. Sci. **5**, 301 (1975). doi:10.1146/annurev.ms.05.080175.001505
43. E.K. Arushanov, Prog. Crystallogr. Growth Charact. **3**, 211 (1980). doi:10.1016/0146-3535(80)90020-9
44. V.B. Lazarev, V.Y. Schevchenko, Y.H. Greenberg, V.V. Sobolein, *II–V semiconducting compounds* (Nauka, Moscow, Russia, 1978)
45. M. Bushan, A. Catalano, Appl. Phys. Lett. **38**, 39 (1981). doi:10.1063/1.92124
46. J.M. Pawlikowski, Infrared Phys. **29**, 177 (1988). doi:10.1016/0020-0891(88)90007-3
47. M.P. Bichat, J.L. Pascal, F. Gillot, F. Favier, Chem. Mater. **17**, 6761 (2005). doi:10.1021/cm0513379
48. E.A. Fagen, J. Appl. Phys. **50**, 6505 (1979). doi:10.1063/1.325746
49. W.E. Buhro, Polyhedron **13**, 1131 (1994). doi:10.1016/S0277-5387(00)80250-8
50. M. Green, P. O'Brien, Chem. Mater. **13**, 4500 (2001). doi:10.1021/cm011009i
51. C. Yan, J. Liu, F. Liu, J. Wu, K. Gao, D.F. Xue, Nanoscale Res. Lett. **3**, 473 (2008). doi:10.1007/s11671-008-9193-6
52. G.Z. Shen, Y. Bando, C. Ye, X. Yuan, T. Sekiguchi, D. Golberg, Angew. Chem. Int. Ed. Engl. **45**, 7568 (2006). doi:10.1002/anie.200602636
53. M. Omari, N. Kouklin, G. Lu, J. Chen, M. Gajdardziska-Josifovska, Nanotechnology **19**, 105301 (2008). doi:10.1088/0957-4484/19/10/105301
54. C. Liu, L. Dai, L.P. You, W.J. Xu, R.M. Ma, W.Q. Yang, Y.F. Zhang, G.G. Qin, J. Mater. Chem. **18**, 3912 (2008). doi:10.1039/b809245a
55. G.Z. Shen, Y. Bando, D. Golberg, J. Phys. Chem. C **111**, 5044 (2007). doi:10.1021/jp068792s
56. R. Yang, Y.L. Chueh, J.R. Morber, R. Snyder, L.J. Chou, Z.L. Wang, Nano Lett. **7**, 269 (2007). doi:10.1021/nl062228b
57. C. Xu, S. Youkey, J. Wu, J. Jiao, J. Phys. Chem. C **111**, 12490 (2007). doi:10.1021/jp0730794
58. J. Jie, W. Zhang, Y. Jiang, X. Meng, J.A. Zapien, M. Shao, S.T. Lee, Nanotechnology **17**, 2913 (2007). doi:10.1088/0957-4484/17/12/015
59. G.Z. Shen, Y. Bando, B. Liu, C. Tang, D. Golberg, J. Phys. Chem. B **110**, 20129 (2006). doi:10.1021/jp057312e
60. H.W. Kim, S.H. Shim, Thin Solid Films **515**, 5158 (2007). doi:10.1016/j.tsf.2006.10.043
61. X. Tao, X.D. Li, Nano Lett. **8**, 505 (2008). doi:10.1021/nl072678j
62. K. Zou, X. Qi, X. Duan, S. Zhou, X. Zhang, Appl. Phys. Lett. **86**, 013103 (2005). doi:10.1063/1.1844041
63. G.Z. Shen, P.C. Chen, Y. Bando, D. Golberg, C. Zhou, Chem. Mater. **20**, 7319 (2008). doi:10.1021/cm802516u
64. G.Z. Shen, P.C. Chen, Y. Bando, D. Golberg, C. Zhou, J. Phys. Chem. C **112**, 16405 (2008). doi:10.1021/jp806334k
65. G.Z. Shen, Y. Bando, J.Q. Hu, D. Golberg, Appl. Phys. Lett. **88**, 143105 (2006). doi:10.1063/1.2192090
66. G.Z. Shen, C. Ye, D. Golberg, J. Hu, Y. Bando, Appl. Phys. Lett. **90**, 073115 (2007). doi:10.1063/1.2539821
67. C. Liu, L. Dai, R.M. Ma, W.Q. Yang, G.G. Qin, J. Appl. Phys. **104**, 034302 (2008). doi:10.1063/1.2960494